Chem Catalysis

CellPress

Article

A Bioinspired Approach towards Efficient Supramolecular Catalysts for CO_2 Conversion

Ferran Esteve,[1,2,] Raúl Porcar,[2,3] Michael Bolte,[4] Belén Altava,[2] Santiago V. Luis,[2] and Eduardo García-Verdugo[2,5,*]

[1]*Dpt. of Inorganic and Organic Chemistry, Supramolecular and Sustainable Chemistry Group, University Jaume I, Avda Sos Baynat s/n, E-12071-Castellon, Spain.*

[2]*Laboratoire de Chimie Supramoléculaire, Institut de Science et d'Ingénierie Supramoléculaires (ISIS), Université de Strasbourg, 8 allée Gaspard Monge, Strasbourg, 67000, France*

[3]*Dpt. of Organic and Bioorganic Chemistry, Universidad Nacional de Educación a Distancia, Avda. Esparta, 28232-Las Rozas, Madrid, Spain.*

[4]*Institute of Inorganic Chemistry, Goethe University Frankfurt, Max-von-Laue-Straße 7, 60438 Frankfurt am Main, Germany.*

[5]Lead contact

*Correspondence: cepeda@uji.es

SUMMARY

Nature uses enzymes for affording astonishingly efficient chemical transformations with high chemo-, regio-, and stereoselectivity (*e.g.*, carbonic anhydrase for CO_2 conversion). Such sophisticated biomolecules lead to excellent catalytic activities as a result of harmonized supramolecular interactions with the substrates/intermediates of the reactions. Based on this approach, different Zn^{2+} complexes of pseudopeptidic macrocycles with a high level of preorganization were synthesized and tested as catalysts for the cycloaddition of CO_2 to epoxides. These bioinspired systems promoted remarkable activities even at mild conditions, without the need of any auxiliary co-catalysts. The whole catalytic cycle was dominated by cooperative non-covalent forces involving multiple functional sites, displaying an enzyme-like catalytic behaviour. Besides, the chiral environment associated to the amino acid sidechains in the preorganized catalytic system provided recognition sites for efficient kinetic resolution of epoxides. In the case of the sluggish styrene oxide substrate, the highest selectivity factor reported to date was attained.

Supramolecular catalysis, pseudopeptides, bioinspired chemistry, macrocyclic compounds, CO_2 conversion, cyclic carbonates, one-component catalysts

INTRODUCTION

One of the major challenges facing the global chemical community is reducing atmospheric carbon dioxide.[1] Fortunately, CO_2 can be seen as a cheap, abundant, and nontoxic substance that can lead, in combination with other simple molecules, to added-value chemical products, offsetting the energetic and economic costs of CO_2 capture.[2] Still, its valorisation requires the development of effective catalysts to overcome the low reactivity of CO_2.[3] In this regard, enzymes pave the way for an effective and controlled activation and conversion of CO_2 under moderate conditions, as evidenced during cellular metabolism.[4,5] However, several critical issues hamper the industrial implementation of such enzymatic systems.[6] Therefore, the design of new active and stable catalysts able to mimic enzymatic behaviours using similar supramolecular interactions is of high interest for CO_2 transformation.[7,8,9]

Among the different added-value products that have been obtained using CO_2, cyclic carbonates (CC) are one of the most popular due to their numerous industrial applications.[10] CC can be obtained through CO_2 cycloaddition to epoxides, though one may realize that this transformation can only account for a minor amount of overall carbon dioxide emissions. The

The bigger picture

Enzymes employ elegant catalytic pathways to provide astonishing efficiencies in catalytic transformations. Such high activities are a direct consequence of cooperative supramolecular interactions between the optimally arranged amino acid residues of the biomolecule and substrates/intermediates of the chemical reaction. Inspired by this approach, we present herein highly preorganized supramolecular catalysts for the cycloaddition of CO_2 to epoxides, a key reaction for the conversion of CO_2 into added-value products. The pseudopeptidic complexes can activate substrates and stabilize reaction intermediates through non-covalent forces, with remarkable activities under mild conditions and in the absence of auxiliary co-catalysts. Besides, the presence of a rigidized chiral cavity surrounding the active site permitted to attain high *s* factors for the kinetic resolution of styrene oxide. We believe that these finding will be a major asset towards designing highly active enzyme-like supramolecular catalysts for challenging CO_2 transformations.

most common catalytic approach being the use of monofunctional catalysts (Lewis acids or bases) in combination with nucleophiles that act as co-catalysts (Figure 1A).[11] In such systems, Lewis acid centres activate the C-O bond of the epoxide (Figure 1A1), whereas the presence of Lewis bases facilitates CO_2 activation (Figure 1A2).[12,13,14] For both homogeneous and heterogeneous catalysts of this class, supramolecular chemistry approaches have revealed advantageous as much as the formation of host-guest complexes between the two components efficiently enhances the catalytic performance.[15,16,17,18] However, such systems often operate in the presence of a huge excess of co-catalysts, increasing the waste generated in the process.[19]

In this regard, the design of bifunctional systems not requiring any additional co-catalyst is a greener and more bioinspired aproach, representing a current hot topic.[20,21] The active sites are part of the same molecule, being linked through chemical spacers that can modulate the conformational features of the final catalytic species (Figure 1B).[22,23,24,25,26,27] Nonetheless, attaining optimally preorganized scaffolds involves the use of complex structures that require multistep syntheses and tedious purification protocols.[28] In addition, most of these bifunctional systems still suffer from low activity at mild conditions (*i.e.*, room temperature and 1 bar of pressure), needing high catalyst loadings to achieve good conversions.[29]

Inspired by all these precedents, we envisaged that a suitable design of macrocyclic pseudopeptidic Zn(II)-complexes could promote major advantages in this research field. We report herein the synthesis of a series of multifunctional bimetallic complexes and their use as multifunctional supramolecular catalysts. The conformationally constrained macrocyclic structure rendered an optimal spatial distribution for cooperation between all active sites: Lewis acidic groups (Zn^{2+}, amide groups, and acidic hydrogen atoms of the coordinated amines), Lewis basic groups (amino groups), and activated nucleophiles (iodide counterions). The strong synergic effect between the different functionalities led to remarkable results in terms of activity and even enantioselectivity, with the catalytic mechanism being governed by supramolecular interactions (Figure 1C). This catalytic behaviour mimics the mode of action observed during enzymatic transformations, in which optimally arranged amino acid residues and cofactors lead to superb activities (Figure 1D).[30]

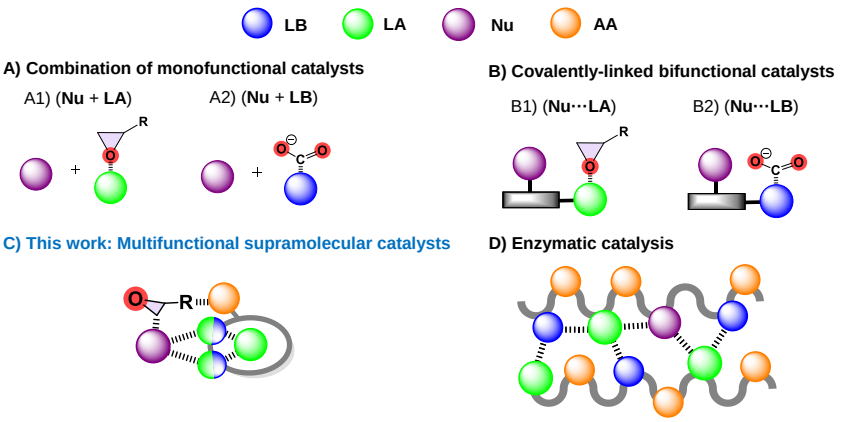

Figure 1. Schematic representation for the proposed approaches in the catalytic cycloaddition of CO_2 to epoxides and the design inspired from enzymes.

[LA = Lewis acid site, LB = Lewis base, Nu = nucleophile, and AA = amino acid sidechains].
(A) Monofunctional catalysts in the presence of a nucleophilic co-catalyst.
(B) Covalently-linked bifunctional catalysts.
(C) Multifunctional supramolecular catalysts here described.
(D) Enzymatic catalysis.

RESULTS AND DISCUSSION

The new family of macrocyclic compounds was synthesized *via* imine condensation of the open-chain C_2-pseudopeptidic bisaminoamides (**B**) with 5-(tert-butyl)-2-hydroxyisophthalaldehyde (**DA**) followed by *in-situ* reduction (Scheme 1). The dynamic nature of the imine bonds allowed for the formation of the thermodynamically favoured [2+2] macrocycles, overcoming the production of side products of oligomeric/polymeric

nature.[31] The high efficiency of the macrocyclization reaction is the result of the higher thermodynamic stability of these cyclic constituents, likely due to stabilizing intramolecular hydrogen bonds between the amide groups of the pseudopeptidic chains as facilitated by the aprotic apolar solvent used ($CHCl_3$).[32] Indeed, when the condensation reaction was carried out with 1,8-diaminooctane, instead of the pseudopeptides **B**, the formation of oligomers/polymers was observed. This is in agreement with the postulated attractive hydrogen bonds associated to the amide groups (Figure S1).[33] It must be highlighted that high isolated yields were achieved for all pseudopeptidic macrocycles, without the need of using auxiliary templating agents (Table S1), even at relatively high concentrations (30 mM).[34] Crystals suitable for X-ray diffraction measurement were grown for the protonated **L1** macrocycle (**H_2L1**). The solid-state structure revealed a highly twisted conformation involving intramolecular ($d_{HN\cdots OC}$ = 2.78 Å, 92% $vdW_{N,O}$) and intermolecular ($d_{HN\cdots OC}$ = 2.94 and 2.84 Å, 96 and 93% $vdW_{N,O}$, respectively) hydrogen bonds between the amide groups of the pseudopeptidic chains (Figure S2), corroborating the effect of such interactions in thermodynamically favouring the formation of [2+2] macrocycles.[35]

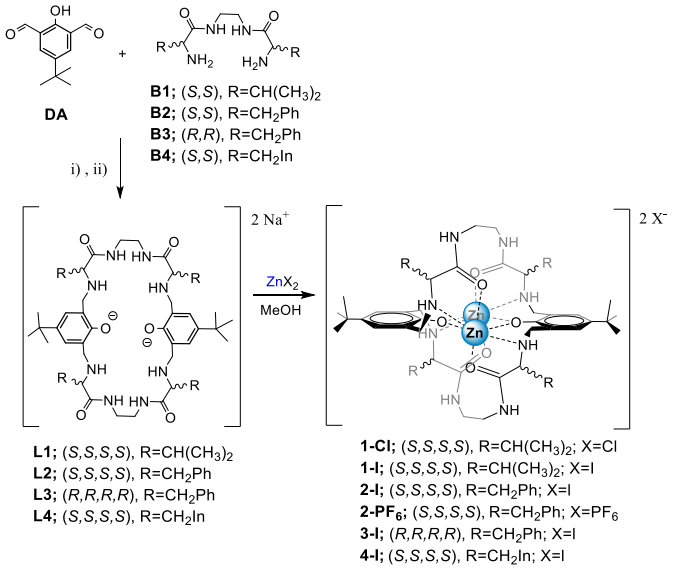

Scheme 1. Synthetic route to produce the pseudopeptidic macrocycles L1-L4 and their Zn^{2+} complexes 1-4.

(i) $CHCl_3$ (30 mM concentration for each reagent), Na_2SO_4 at 25 ºC for 15 h. (ii) MeOH, $NaBH_4$ excess at 25 ºC for 2 h. The metal-complexation step was carried out at 25 ºC. Isolated yields for the different steps are summarized in the experimental section.

The sodium salts of macrocycles **L1-L4** were then reacted with ZnX_2 salts, leading to the formation of the corresponding bimetallic pseudopeptidic complexes **1**-**4** with yields in the 80-90% range (Scheme 1). The solid-state structure of **4-I** provided unambiguous evidence for complex formation (Figure 2A). While the two phenoxy-groups act as bridges between the two Zn cores, one amino group of each pseudopeptidic moiety completes the equatorial coordination plane of the metal (Figure 2B), as previously reported for related macrocyclic systems.[36,37] In this pseudopeptidic system, in contrast to formerly reported molecular structures, the counterions are not directly coordinated to the metallic sites. Instead, two oxygen atoms from two amide groups are further coordinated to the apical positions of each metallic centre, resulting in a distorted octahedral coordination sphere for each Zn^{2+} (Figure 2B). Consequently, the iodide anions are located in a preorganized chiral 3D-cavity defined by the constrained pseudopeptidic sidechains (Figure 2A), stabilized by hydrogen bonds with the acid hydrogen atoms of the coordinated secondary amines ($d_{N\cdots I}$ = 3.69 Å, 105% $vdW_{N,I}$). The crystal structure of **4-I** exhibits an extremely long zinc-iodide average distance of 4.49 Å (Figure 2B).

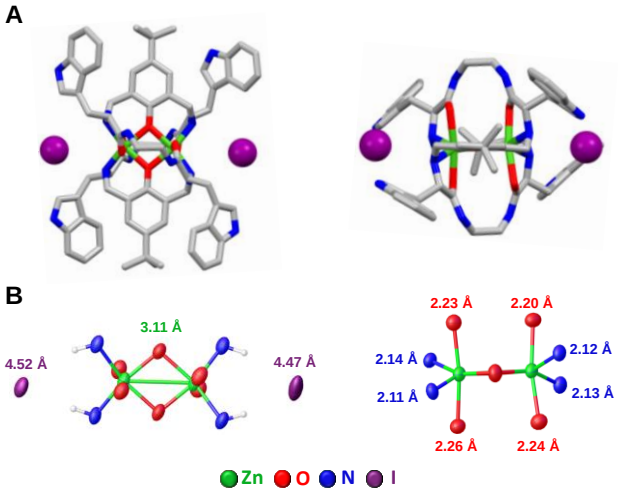

Figure 2. Solid-state structure for 4-I.

(A) Side and top view of the supramolecular structure found. Hydrogen atoms and solvent molecules have been removed for clarity. Iodide anions are highlighted in violet.
(B) Representation of the distorted octahedral coordination spheres for Zn^{2+} ions. Distances between atoms and metallic cores have been highlighted in different colours. The intermetallic Zn-Zn distance has been marked in green.

Preliminary information on the potential catalytic activity of the considered metal complexes for the cycloaddition of CO2 to epoxides was obtained from compounds **1-Cl** and **1-I** (Table 1). The reaction between styrene oxide (SO) and CO_2 under solvent-less conditions was selected as the benchmark reaction (Scheme 2). Table 1 summarises the results obtained for the different conditions assayed.

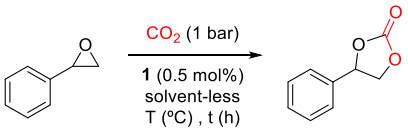

Scheme 2. Cycloaddition of CO_2 to SO in the presence of catalyst 1

Table 1. Catalytic results obtained for zinc complexes 1-Cl and 1-I in the cycloaddition of CO_2 to styrene oxide under solvent-less conditions

Entry	Cat. (mol%)[a]	Temp. (ºC)	Time (h)	Conv. (%)[b]
1	ZnI_2 (1)	100	3	14
2	ZnI_2 (1)	100	1	3
3	$ZnCl_2$ (1)	100	3	0
4	**1-I** (0.5)	100	3	>99
5	**1-I** (0.5)	100	1	>99
6	**1-Cl** (0.5)	100	3	53
7	**1-I** (0.5)	80	1	>99
8	**1-Cl** (0.5)	80	3	14
9	**1-I** (0.5)	60	3	90
10	**1-I** (0.5)	60	1	31
11	**1-I** (0.5)	40	3	14
12	**1-I** (0.5)	r.t.	15	23

[a]Reaction conditions: styrene oxide (4.35 mmol), 1 bar of CO_2 (autoclave).
[b]Conversions determined by ^{1}H NMR, selectivity for styrene carbonate was always > 99% when using pseudopeptidic complexes. Formation of side-products (mainly diol species) was detected when using ZnI_2.

Complex **1-I** showed a remarkable activity, leading to quantitative conversions in only 1 h at 100 ºC (entry 5, Table 1) with a TOF value of 198 h^{-1}, while the zinc salts in the absence of macrocyclic ligand showed low or no activity at the same temperature (entries 1-3, Table 1). When **1-Cl** was used, the performance suffered a significant decrease (entry 6, Table 1). This activity decrease was assigned to the lower nucleophilicity of chloride anions, which might also be more strongly hydrogen-bonded to the acidic hydrogen atoms of the pseudopeptidic structure as a result of its higher charge density. As expected, lower temperatures afforded lower conversions into the desired styrene carbonate (SC) for **1-Cl** (entry 8, Table 1). Notwithstanding, **1-I** still afforded a quantitative conversion at 80 ºC in 1 h and a 90% conversion in only 3 h of reaction at 60 ºC (always at 1 bar of CO_2), which represents an extraordinary value considering the moderate reactivity of SO (entries 7 and 9, Table 1). This valine-derived catalyst was found to be active even at room temperature, obtaining a 23% conversion, with excellent selectivity, after 15 h of reaction (entry 12, Table 1). These results highlight the exceptional activity of these pseudopeptidic multifunctional complexes, taking into account that they work in the absence of any auxiliary co-catalyst.

According to these results, **1-I** shares with enzymes the capacity of being active under mild conditions, but also the presence of a well-defined chiral environment, which potentially could be used to provide enantiodiscrimination during the cycloaddition of CO_2 to SO. Chiral epoxides and cyclic carbonates are important intermediates in the production of pharmaceutical and biological compounds.[38,39] These enantiopure species are traditionally prepared by the cyclization of chiral diols with highly toxic triphosgene.[40,41] In the search of less hazardous methodologies, the kinetic resolution of racemic epoxides in the presence of carbon dioxide has been exploited, as this is a greener alternative presenting 100% atom economy.[19,42,43,44,45,46,47] A limited success has been achieved in this regard, as a main hurdle for such approach is the harsh conditions often required for overcoming the inertness of CO_2, which in turn adversely affects the enantiomeric excess of the final carbonate.[48] Thus, we decided to evaluate the potential of the macrocyclic complex (**1-I**) for the kinetic resolution of racemic SO. GC analyses allowed for the quantification of the enantiomeric excess for SC. The use of enantiomerically enriched SO mixtures confirmed that a kinetic resolution of racemic oxiranes was occurring (Figure S3). At 40 ºC, 0.5 mol % of **1-I** and 1 bar CO_2, conversions after 15 hours increased with the initial amount of the *R*-enantiomer present in the mixture. Indeed, conversions ranged from 7% for pure *S*-enantiomer to 19% for pure *R*-enantiomer, indicating a faster reaction with (*R*)-SO. In addition, for those enantioenriched mixtures, the percentage of (*R*)-SC found was always higher than the percentage of the *R*-enantiomer in the starting SO, corroborating the kinetic resolution of racemic SO.

Table 2. Effect of the amino acid side chain on the catalytic kinetic resolution of styrene oxide by CO_2 cycloaddition under solvent-less conditions and catalysed by zinc iodide-pseudopeptidic macrocycles complexes

Entry	Cat.[a]	Temp. (ºC)	Time (h)	Conv. (%)[b]	*e.e.* (%)[c]	s[f]
1	**1-I**	60	1	31	21[d]	2.4
2	**2-I**	60	1	38	30[d]	2.2
3	**4-I**	60	1	15	12[d]	1.9
4	**1-I**	40	4	14	39[d]	2.4
5	**2-I**	40	4	27	58[d]	4.6
6	**4-I**	40	4	9	29[d]	1.9
7	**3-I**	40	4	25	56[e]	4.2
8	**1-I**	r.t.	15	21	49[d]	3.3
9	**2-I**	r.t.	15	23	68[d]	6.4
10	**4-I**	r.t.	15	6	34[d]	2.0
11	**2-I**[g]	r.t.	15	52	55[d]	6.2
12	**2-I**	r.t.	24	45	69[d]	9.5
13	**2-I**	100	2	XX	n.d.	n.d.

[a]Reaction conditions: styrene oxide (4.35 mmol), 0.5 mol% of catalyst, 1 bar of CO_2 (autoclave).

[b]Conversions determined by ^{1}H NMR, selectivity for styrene carbonate was always > 99%.

[c]Enantiomeric excess determined by GC analyses.

[d]Enantiomeric excess for (*R*)-styrene carbonate.
[e]Enantiomeric excess for (*S*)-styrene carbonate.
[f]*s* = ln[(1-c(1+ee)]/ln[1-c(1-ee)], where c is the conversion and ee is the enantiomeric excess.
[g]1 mol% of catalyst.
n.c. = not determined.

The considered macrocyclic structures, as well as their corresponding Zn complexes display a highly modular character based on the nature of the component amino acids, an approach that has been fruitfully exploited by Nature. Thus, we examined the effect of the nature of the pseudopeptidic sidechains. Results in Table 2 illustrate that the amino acid residue was clearly affecting to both activity and enantiopreference of the process. In terms of the catalytic activity, the observed trend was Phe > Val > Trp (**2-l** > **1-l** > **4-l**, entries 1-10, Table 2) with best results detected for the phenylalanine-derived bimetallic complex **2-l**. This suggests the involvement of π-interactions in the reaction mechanism, likely stabilizing transition states / reaction intermediates (*vide infra*). Increasing the catalytic loading of **2-l** to 1 mol%, a 52% yield could be achieved after 15 h of reaction at room temperature (entry 11, Table 2). In the light of the remarkable activity provided by **2-l**, we decided to perform an additional experiment at 100 ºC and 1 bar of CO_2, with a catalytic loading of 0.1 mol% for **2-l** (Entry 13, Table 2). After 2 hours of reaction, the system afforded TON and TOF values of 650 and 325 h^{-1}, respectively, corroborating the high activity of the catalyst even for such a sluggish substrate (*i.e.,* SO).[49] Regarding the enantioselectivity attained, the kinetic resolution efficiency increased as the temperature decreased, following the trend **2-l** > **1-l** > **4-l**. Also in this regard, **2-l** afforded best results. Incrementing the reaction time to 24 h at room temperature resulted in an *s*-factor as high as 9.5 for **2-l** (Entry 12, Table 2). To the best of our knowledge, this is the highest *s*-factor reported to date for the kinetic resolution of styrene oxide (see Figure S4 and Table S2). When the macrocyclic complex **3-l** displaying the (*R,R,R,R*) configuration was used, the formation of (*S*)-SC was instead favoured (Table 2, compare entries 5 and 7) affording *e.e.* and *s*-factor values similar to those found for **2-l**.
Different terminal epoxides were then studied for the formation of their respective cyclic carbonates in the presence of CO_2 and **2-l** (Table S3). At 80 °C and under 1 bar of CO_2, all epoxides were smoothly converted into the desired organic carbonates with excellent conversions (> 90%). In addition, complex **2-l** was able to promote efficient kinetic resolutions with enatioselectivities of *ca*. 40% *e.e.* and *s*-factors of 2.4-2.9 at 40 °C for the different substrates assayed. It must be highlighted that the use of glycidyl phenyl ether as substrate (entries 5 and 6, Table S3) led to a significant decrease in the conversion in comparison with SO (entries 1 and 2, Table S3). This activity drop is in accordance with the proposed essential role of π-π interactions, as the ether substitution on the aromatic ring (electron donating group) reduces the affinity to form such supramolecular forces with the already electron-rich aromatic unit of the pseudopeptidic sidechains.
Based on the remarkable activities obtained and the solid-state structure of the complex (Figure 2), we can propose that the crowded coordination sphere of the Zn^{2+} metallic cores allowed for the presence of highly nucleophilic iodide anions. These "naked" anions rendered an extremely efficient ring-opening step, explaining the excellent activities observed.[15] The synergies between the metallic core and the "naked" iodide anion were demonstrated by additional catalytic experiments (Table S4). The parent unit **L2**, lacking both the nucleophile source and Zn^{2+} centres, did not promote the formation of styrene carbonate. Addition of 1 mol% of iodide anion as its tetrabutylammonium salt in the presence of 0.5 mol% of **L2** only resulted in a 2% conversion, suggesting that the metallic core is of paramount importance for the activation of the substrates under such mild reaction conditions. In the same way, when **2-PF_6** was used in the reaction, only minor traces of SC were detected. This result indicates that the presence of an activated nucleophile is a requirement for triggering the catalytic cycle. All this evidence reflects that the observed activity and enantioselectivity involve a tight cooperativity between the different catalytic sites of the supramolecular system, all preorganized in an optimal spatial disposition within the chiral complex (Figure 1). This catalytic behaviour mimics the sophisticated cooperative non-covalent interactions used by Nature in enzymatic transformations.[30]
Several spectroscopic experiments were then designed for gaining additional insights into mechanistic aspects. The reaction order for **2-l** was determined by *in-situ* FTIR spectroscopy at 60 ºC in the presence of a CO_2 balloon (Figure S5).[50] The aftermath of the kinetic study revealed a first-order dependence on the bimetallic catalytic species (Figures S6 and S7).[51]

Conformational information was gathered by measuring ^{1}H NMR spectra for **2-I** in different solvents. Figure 3 shows that the structure of the complex is conformationally very rigid, as demonstrated by the noteworthy anisochrony observed for the diastereotopic Ar-CH_2-NH_{amine} methylene protons (orange signals in Figure 3). Besides, in the presence of solvents containing Lewis basic groups, the signals for the amide protons (green signals in Figure 3) appeared at higher δ values, following the expected basicity trend (DMSO > acetone > THF >> ACN). This observation can be explained by the formation of hydrogen bonds between the acidic amide protons and the basic donor sites of the solvents, as also observed in the solid-state structure of **4-I** (Figure S8).[52]

The acidic proton signals for the coordinated secondary amines (red spheres in Figure 3) did not respond to such basicity trend. Instead, they appeared at much lower fields in the presence of THF/acetone than in DMSO. Comparing the shifts with the ones obtained for the barely preorganized conformation in acetonitrile, $\Delta\delta$ values of +1.8, +1.5, and +0.2 ppm were found for the NH_{amine} signals in THF, acetone, and DMSO, respectively. These differences can be assigned to the polarity of the solvents. For instance, DMSO presents a higher relative polarity than THF (0.444 *vs* 0.207 relative polarity to water).[53] This might lead to a better solvation for the iodide counterions as suggested by the higher fields observed for the amino group protons that are less influenced by the electronegative anions in the most polar solvents like DMSO and ACN (Figure 3). On the other hand, poor solvation of the negatively charged iodide ions results in tight hydrogen bonding with the acidic protons of the coordinated amines (see Figure 3 and Figure S8). These non-covalent interactions between the anions and the amine hydrogen atoms confers additional rigidity to the whole structure of the bimetallic pseudopeptidic complex, as corroborated by the significantly different electronic environment experienced by the aromatic protons of the phenylalanine side chains in THF and acetone (blue signals, Figure 3). Considering the structural similarities between THF and oxiranes, one may realize that the catalytically active conformation of the pseudopeptidic complexes in SO must be like the one found in THF. Indeed, ^{1}H NMR titration experiments of **2-I** with styrene oxide and THF showed similar chemical shift variations (Figure S9), corroborating this assumption. Therefore, the efficiency of the catalyst in the kinetic resolution of epoxides could be explained by the rigidized chiral sidechains of the complex that are located in the surroundings of the activated nucleophilic anion (see Figure 1 for representation).

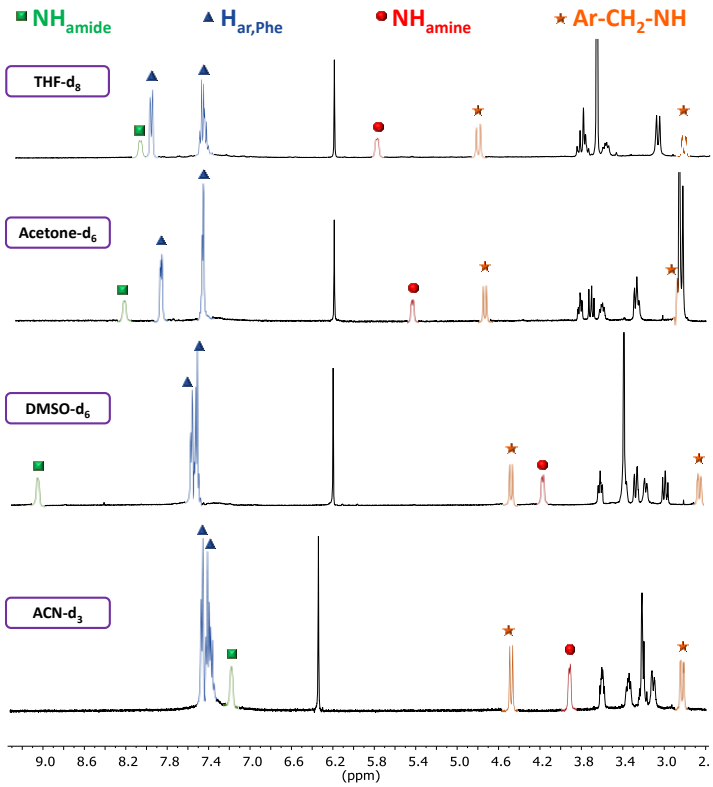

Figure 3. Partial ^{1}H NMR spectra of 2-I in different deuterated solvents.

^{1}H NMR spectra acquired at 400 MHz and 25 ºC for **2-I** (2 mM). From top to bottom: deuterated THF, acetone, DMSO, and ACN used as solvents, respectively. The signals for the protons discussed in the text have been highlighted with different colours.

The capability of the pseudopeptidic complex for supramolecular recognition was assayed in the presence of the two enantiomers of the substrate, namely (*S*)-SO and (*R*)-SO. The association constants for the equimolecular **2-I** : SO system, as determined by ^{1}H NMR titration experiments, revealed a preferential recognition of (*R*)-SO over its (*S*)-enantiomer (Figures S10 and S11). This observation could be the result of the formation of attractive π-π interactions between the pseudopeptidic sidechain and the aromatic moiety of (*R*)-SO, likely unattainable in the case of (*S*)-SO (see Figure 5c). One may realize that this favoured recognition of one of the enantiomers (binding constants of 16 ± 1 M^{-1} and 8 ± 1 M^{-1} respectively for (*R*)-SO and (*S*)-SO, Figures S10 and S11) could be even more pronounced in the supramolecular complexation of the reaction intermediates and transition states (*vide infra*), explaining the high enantioselectivity observed in the transformation (see, for instance, entry 12, Table 2). Conformational changes for **2-I** in the presence of (*R*)-SO were also monitored using circular dichroism (CD). Interestingly, a significant decrease was observed in the intensity of the negative band centred at 215 nm -absorption of amide groups- upon addition of (*R*)-SO (Figure 4A).[54] This result is consistent with a change in the chiral environment of the amide moieties upon hydrogen bonding with the basic oxygen atom of the epoxide.[17] As expected for this supramolecular recognition process, a red-shift was concomitantly detected in the UV absorption signal for the amide band (orange arrow, Figure 4B).

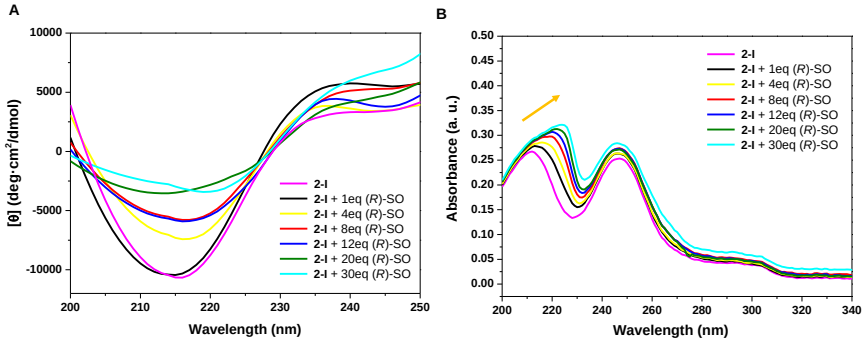

Figure 4. CD and UV-Vis spectra for the titration of 2-I with increasing amounts of (*R*)-SO

A) CD spectra (CH_3CN, 25 ºC) for the titration of **2-I** (0.01 mM) with increasing amounts of (*R*)-SO.

B) UV-Vis spectra (CH_3CN, 25 ºC) for the titration of **2-I** (0.01 mM) with increasing amounts of (*R*)-SO. The red-shift observed for the amide band has been highlighted with an orange arrow

The concentration of the organometallic host was maintained constant during the experiment.

The potential capacity of these complexes to activate carbon dioxide molecules was also studied by ^{1}H NMR and ESI-MS. The presence of amino groups in the macrocyclic structure could result in activation of carbon dioxide molecules.[55,56,57] Albeit we did observe some sort of reversible interaction between the pseudopeptide and carbon dioxide at high CO_2 pressures (10 bar; Figures S12-S16), these conformational changes were minor at 1 bar CO_2 pressure. This, together with the surmised high efficiency in the ring-opening step triggered by the "naked" iodide anions, suggested that the most feasible catalytic pathway is the CO_2 molecule being directly fixed by a nucleophilic attack of the highly reactive alkoxylate intermediate formed after the epoxide ring-opening (**A2** in Figure 5A).

All these data allow for the postulation of a plausible mechanism for the catalytic CO_2 conversion in the presence of SO and **2-I** (Figure 5A). After the preferent recognition of (*R*)-SO by the Zn^{2+} complex (adduct **A1**), the "naked" iodide anion attacks to the α-C of the oxirane, as previously reported for aromatic epoxides.[58] This initial step led to the alkoxylate intermediate, which can be stabilized by means of hydrogen bonds with the acidic hydrogen atoms of the Zn-coordinated NH groups (**A2**). Such non-covalent stabilization between the alkoxylate anion and two hydrogen bond donor groups of the pseudopeptide resembles the oxyanion holes found in enzymes, as previously described for analogous systems.[59] Additional hydrophobic interactions with the amino acid residues could further stabilise this intermediate. At this point, nucleophilic attack of the alkoxylate to the electrophilic carbon of the CO_2 molecule allowed for the formation of the carboxylate **A3** that can also be stabilized through hydrogen bonding with the hydrogen atoms of the Zn-coordinated secondary amino groups. In the last step, the intermediate **A3** experiences a ring-closing step, yielding the desired (*R*)-styrene carbonate (**A4**).

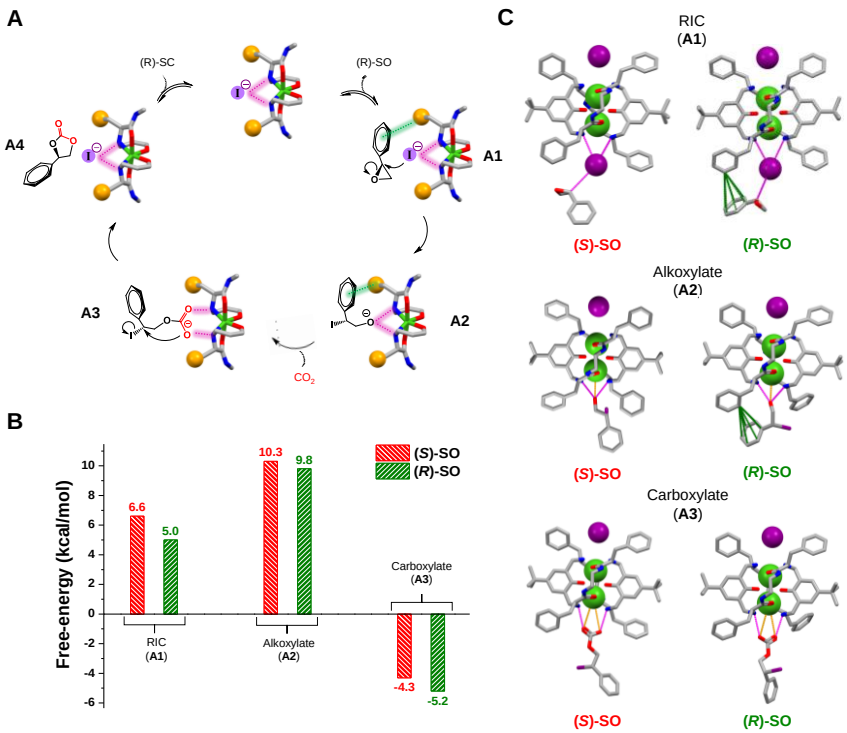

Figure 5. Proposed mechanism and DFT calculations

A) Postulated mechanism for the enantioselective cycloaddition of CO_2 to styrene oxide in the presence of the one-component bimetallic Zn^{2+} catalysts. The symmetry equivalent (half-molecule) of the pseudopeptidic Zn^{2+} complex has been represented with 3D sticks. The sidechains of the amino acid fragments have been represented with orange balls.

B) Free-energies obtained, considering the two initial SO enantiomers, for: RIC (**A1**), alkoxylate (**A2**), and carboxylate (**A3**). Red bars correspond to energies obtained starting from (*S*)-SO and green bars correspond to energies from (*R*)-SO.

C) DFT models (b3lyp/lanl2dz) calculated for the most relevant species involved in the catalytic cycle. Hydrogen bonds highlighted with discontinuous magenta lines. Electrostatic interactions highlighted with discontinuous orange lines. Aromatic interactions highlighted with discontinuous green lines.

Preliminary DFT calculations (b3lyp/lanl2dz) were performed for the two enantiomeric supramolecular adducts of relevant species **A2** and **A3**, as well as for the initial reactants interaction complex (RIC) (**A1** in Figures 5B and 5C). Free-energies were determined taking the energies of the catalyst **2-I** and each of the SO enantiomers as zero. In all cases, the supramolecular species resulting from the reaction with (*R*)-SO were more stable than the ones calculated for the reaction with the (*S*)-enantiomer. As surmised, the preorganization of the different components in the RIC **A1** was facilitated by non-covalent forces, namely hydrogen bonds, electrostatic, and π-π interactions. The endergonic nature of the epoxide recognition process is related with the entropic cost of bringing two molecules together.[58] The preferential interaction with (*R*)-SO was assigned to the presence of attractive edge-to-face aromatic forces (for the closest C_{ar}, $d_{C\text{-}C}$ = 3.99 Å, Figure 5C).[60] Such a favourable interaction was not possible in the presence of (*S*)-SO (see Figures 5B and 5C for conformations and energy differences). A similar scenario was found for the alkoxylate intermediate **A2**, although in this case the intermediate from (*R*)-SO was only favoured by 0.5 kcal/mol. Calculations indicate that one of the sidechains experiences a conformational change relative to the one present in **2-I** for the anionic intermediates (**A2** and **A3**) resulting from (*R*)-SO, most likely to maximize the attractive forces between the catalyst and intermediates.

CONCLUSION

Results here presented highlight the potential and relevance of bioinspired approaches for the development of efficient catalytic systems for CO_2 conversion into added-value chemicals. The appropriate design of pseudopeptidic macrocycles has been demonstrated to lead to compounds able to form binuclear Zn^{2+} complexes with a high level of preorganization. The resulting complexes present a variety of functional groups properly located in close proximity (acidic hydrogen atoms, basic centres, nucleophilic anions not coordinated to the metal centre…) that synergistically cooperate to establish supramolecular interactions. Such structural features have revealed to be essential for their behaviour as efficient catalysts for the cycloaddition of CO_2 to epoxides, as studied experimentally and through computational calculations. The reaction takes place under mild conditions and without the need of any additional co-catalyst, which implements the green and sustainable character of this process. Besides, their pseudopeptidic nature provides them with a high level of modularity that can be simply achieved through the modifications in the sidechain of the component amino acids or thorough the nature of the anion. Some of these catalytic systems can provide quantitative transformations of CO2 and epoxides into the corresponding cyclic carbonates at 80 ºC in 1 h, with catalyst loadings of 0.5 mol% and 1 bar of CO_2. Finally, the intrinsic chiral nature of compounds derived from amino acids and the rigid conformational preorganization of the studied Zn complexes allows to create a chiral environment in the constrained space where the reaction takes place, mimicking the situation found in enzymatic active pockets. Thus, the combination of efficient CO_2 conversions under mild conditions and the presence of the amino acid-based chirality facilitated achieving the kinetic resolution of racemic epoxides, which is not often found in this field.

From the compounds studied in this work, the catalyst derived from phenylalanine and containing the iodide anion (**2-I**) afforded best results, with higher conversions and enantioselectivities than valine and tryptophan analogues. This can be ascribed to the presence of attractive π-π intermolecular interactions with the substrate and reaction intermediates, as corroborated by DFT calculations. Such stabilizing interactions appear to be more efficient for the (*R*)-styrene oxide than for the (*S*) enantiomer, explaining the enantioselectivity observed. At room temperature, **2-I** was able to afford after 24 h (0.5 mol% loading, 1 bar of CO_2) a 45% yield of the carbonate from styrene oxide, with an *s*-factor as high as 9.5, which represents the highest *s*-factor reported to date, to the best of our knowledge, for the kinetic resolution of styrene oxide.

Overall, the high level of structural and functional preorganization that can be achieved with relatively simple macrocyclic pseudopeptides like the one studied in this work, facilitates the preparation of metal complexes with an enzyme-like catalytic behaviour based on a harmonized set of cooperative supramolecular interactions between the substrates and the intermediates (and transition states). Albeit attained catalytic activities cannot yet rival the ones promoted by enzymes, the mode of action of the pseudopeptidic catalysts clearly stresses the essential role of optimally arranged supramolecularly-active sites, showcasing enzymatic behaviours. Additional efforts need to be carried out to improve the catalytic efficiency and the enantioselectivity observed -as to be ready for practical applications-, but the present results are key to open the way for developing new bioinspired catalytic systems (*i.e.,* synzymes) for challenging CO_2 sustainable transformations.

EXPERIMENTAL PROCEDURES

Resource availability

Lead contact

Further information and requests for resources should be directed to and will be fulfilled by the lead contact, Eduardo García-Verdugo (cepeda@uji.es).

Materials availability

All materials generated in this study are available from the lead contact without restriction.

Data and code availability

Data and code generated during this study are available from the lead contact upon request.

Instrumentation and measurements

NMR spectra were recorded on Bruker Avance 400 (400 MHz for ^{1}H and 100 MHz for $^{13}C\{^{1}H\}$), Bruker Avance III plus 400 (400 MHz for ^{1}H and 100 MHz for $^{13}C\{^{1}H\}$), and Bruker Ascend Spectroscope Avance Neo-500 MHz (500 MHz for ^{1}H and 125 MHz for $^{13}C\{^{1}H\}$) instruments. MestReNova 10 software was used for the treatment of the NMR spectra. Chemical shifts are given in ppm. NMR tubes were sealed with Teflon caps to avoid evaporation of solvent and changes in concentration. The coupling constants (J) are listed in Hz. Peaks are described as singlet (s), doublet (d), triplet (t), doublet of doublets (dd) and multiplet (m). Unless otherwise noted, spectra were recorded at 25 °C. . Fourier transform infrared spectra (FT-IR) were recorded using an attenuated total reflection adapter (Jasco). HRMS-ESI (High-Resolution Mass Spectrometry-Electro-Spray Ionisation) mass spectra were recorded by direct injection into a ThermoFisher Exactive Plus EMR Orbitrap mass spectrometer. The CD spectra were recorded on CD-ORD J-1500 (Jasco).

Commercially available chemicals were purchased from Sigma-Aldrich, Alfa Aesar, Fluorochem, TCI and were used without further purification. Solvents and reagents of pharmaceutical grade quality were purchased from Carlo Erba, and solvents of spectroscopic grade were purchased from Sigma-Aldrich and Fisher Chemical. Deuterated solvents were purchased from Euriso-TOP.

Open-chain pseudopeptidic precursors (**B1-4**) were prepared following literature procedures.[32]

General procedure for the cycloaddition of CO_2 to styrene oxide

8.7 mmol of epoxide and 0.0044 mmol (or 0.0087 mmol for 1 mol% experiments) of the catalyst were loaded into a Berghof R-300 high-pressure reactor. The reaction vessel was then connected to a pressurized CO_2 source and a back-pressure regulator. The system was purged with 2 bar of CO_2 for 5 minutes, and the final pressure was adjusted to 1 bar. Subsequently, the reaction temperature was risen to the desired temperature and kept at that temperature for the desired time, at 200 rpm stirring. After reaction, the set-up was cooled down to 30 ºC and the excess of CO_2 was released carefully. At the end of the reaction, an aliquot (20 µL) of the resulting mixture was analysed by ^{1}H NMR spectroscopy to determine the conversion and by chiral GC to determine the enantiomeric excess of the cyclic carbonate. The experimental procedures were replicated for all experiments. The average deviation of styrene carbonate formation was less than 5%

General procedure for the ^{1}H NMR conversion determination

^{1}H NMR spectra were recorded by diluting 20 µL of the reaction crude with 580 µL of $CDCl_3$. The signals δ (ppm) for SO are: 2.76 (t, 1H), 3.10 (t, 1H), and 3.82 (t, 1H) for the CH and CH_2 groups and 7.22–7.38 (m, 5H) for the phenyl group. The signals δ (ppm) for the cyclic styrene carbonate are: 4.29 (t, 1H) and 4.82 (t,1H) for the CH_2 (methylene), 5.70 (t, 1H) for the CH (methine), and 7.22–7.38 (m, 6H) for the phenyl group. The conversions were measured by NMR integration, considering the signals at 5.70 and 3.82 ppm for SO and SC, respectively (see Figure S17 for an example).

General procedure for enantiomeric excess determination by GC

The enantiomeric purities for the cyclic carbonates were determined by GC using a chiral column (SUPELCO 24304 β-cyclodextrin120, 30 x 0.25 x 0.25 FILM). The samples were prepared diluting 10 µL of the reaction crude with 990 µL of CH_3CN. The peak at 30.9 min was assigned to (*R*)-SC and the peak at 31.2 min was assigned to (*S*)-SC. The peaks of the initial styrene oxide enantiomers appeared at 11.9 min and 12.1 min for (*R*)-SO and (*S*)-SO, respectively. See GC enantiomeric excess determination section for more details.

General procedure for the IR kinetic experiments

In-situ FTIR spectra were measured for the different solvent-less kinetic experiments. The temperature (60 ºC) was controlled using a Peltier plate, and the CO_2 atmosphere was introduced with a balloon (see Figure S5 for experimental set-up). The data collection consisted of measuring an IR spectrum every 5 minutes. The conversions were determined using an appropriate calibration curve.

General procedure for the spectroscopic titration experiments

The ^{1}H NMR (400 MHz) titration experiments were performed by consecutive additions of the guest to a solution of the desired host. The concentration of the host was kept constant

during the experiment. The association constants were determined using HypNMR software.[61]

Crystal structures

Single crystals suitable for X-ray crystallography were obtained by slow evaporation of a methanol solution of **H_2L1**. A suitable crystal was selected and mounted on a SuperNova, Dual, Cu at zero, Atlas diffractometer. The structure was solved with the SHELXT 2014/5[62] structure solution program and refined with the SHELXL-2018/3[63] refinement package. Artwork representations were processed using MERCURY software.[64] The refined structure of **H_2L1** has been registered in CCDC with the deposition number: 2153938. See ESI for more details.

Single crystals suitable for X-ray crystallography were obtained for **4-I** by slow evaporation of MTBE in a THF solution of the organometallic complex. The molecular structure was solved and refined as detailed above. The refined structure has been registered in CCDC with the deposition number: 2153936. See ESI for more details.

DFT calculations

DFT calculations were run with Gaussian 09 (revision B.01).[65] The X-ray geometric structure for **4-I** was used as the starting point for building-up the models. Geometry optimizations were carried out without symmetry restrictions at the B3LYP level,[66] using the Lanl2Dz basis set.[67] Analytical frequency calculations were used to characterise each stationary point as a minimum. These calculations, carried out at 298.15 K, also allowed for obtaining the thermal and entropic corrections required to calculate Gibbs free-energy differences. See ESI for energies and more details.

Syntheses of the macrocyclic pseudopeptidic ligands

Synthesis of L1

B1 (0.230 g, 0.891 mmol, 2 eq.) was reacted with 4-tert-Butyl-2,6-diformylphenol (0.192 g, 0.891 mmol, 2 eq.) in the presence of Na_2SO_4, forming a suspension on chloroform (30 mL, 30 mM). After 15 hour of reaction, 10 mL of methanol were added to the reaction crude and a big excess of $NaBH_4$ (16 eq.) was poured into the flask. The resultant white suspension was left stirring at room temperature for 2 hours. After removal of the solvent at reduced pressure, compound **L1** was extracted from the solid using chloroform as solvent to yield a yellowish solid (0.298 g, 0.329 mmol, 74% yield). Characterisation: ^{1}H NMR (400 MHz, $CDCl_3$, 25 °C) δ = 7.45 (s, 4H), 6.90 (s, 4H), 3.67 (s, 8H), 3.42 – 3.31 (m, 4H), 3.23 (d, *J* = 9.0 Hz, 4H), 2.87 (d, *J* = 5.3 Hz, 4H), 1.96 (dt, *J* = 13.1, 6.7 Hz, 4H), 1.16 (s, 18H), 0.87 (d, *J* = 6.9 Hz, 12H), 0.80 (d, *J* = 6.8 Hz, 12H); ^{13}C{^{1}H} NMR (400 MHz, DMSO-d_6, 25 °C) δ = 173.1, 153.5, 139.8, 124.0, 123.9, 66.9, 49.0, 38.2, 33.5, 31.6, 19.3, 18.5; FT-IR (ATR): 3278, 3056, 2958, 1646, 1533, 1458 cm^{-1}. MS-ESI(+) m/z: 865.8 ([M + H]$^+$); 887.7 ([M + Na]$^+$).

Synthesis of L2

L2 (yellowish solid, 1.030 g, 0.936 mmol, 79% yield) was synthesized following the protocol described for **L1** but using **B2** as the pseudopeptidic precursor. Characterisation: ^{1}H NMR (400 MHz, CD_3OD, 25 °C) δ = 7.38 – 6.92 (m, 20H), 6.79 (s, 4H), 3.57 (d, *J* = 12.9 Hz, 4H), 3.43 (d, *J* = 12.9 Hz, 4H), 3.33 – 3.24 (m, 4H), 3.16 – 3.00 (m, 12H), 2.88 (dd, *J* = 13.5, 6.2 Hz, 4H), 2.76 – 2.64 (m, 4H), 1.09 (s, 18H);^{13}C{^{1}H} NMR (400 MHz, CD_3OD, 25 °C) δ = 176.1, 155.2, 142.4, 130.3, 130.2, 127.8, 126.6, 125.3, 64.5, 50.3, 40.3, 39.9, 34.7, 32.1; FT-IR (ATR): 3285, 3060, 2952, 1655, 1525, 1454 cm^{-1}. MS-ESI(+) m/z: 1057.6 ([M + H]$^+$); 1079.8 ([M + Na]$^+$).

Synthesis of L3

L3 (yellowish solid, 0.497 g, 0.452 mmol, 75% yield) was synthesized following the protocol described for **L1** but using **B3** as the pseudopeptidic precursor. Characterisation: ^{1}H NMR (400 MHz, CD_3OD, 25 °C) δ = 7.38 – 6.92 (m, 20H), 6.79 (s, 4H), 3.57 (d, *J* = 12.9 Hz, 4H), 3.43 (d, *J* = 12.9 Hz, 4H), 3.33 – 3.24 (m, 4H), 3.16 – 3.00 (m, 12H), 2.88 (dd, *J* = 13.5, 6.2 Hz, 4H), 2.76 – 2.64 (m, 4H), 1.09 (s, 18H);^{13}C{^{1}H} NMR (400 MHz, CD_3OD, 25 °C) δ = 176.1, 155.2, 142.4, 130.3, 130.2, 127.8, 126.6, 125.3, 64.5, 50.3, 40.3, 39.9, 34.7, 32.1; FT-IR (ATR): 3285, 3060, 2952, 1655, 1525, 1454 cm^{-1}. MS-ESI(+) m/z: 1057.6 ([M + H]$^+$); 1079.8 ([M + Na]$^+$).

Synthesis of L4

L4 (yellowish solid, 0.075 g, 0.060 mmol, 64% yield) was synthesized following the protocol described for **L1** but using **B4** as the pseudopeptidic precursor. Characterisation: ^{1}H NMR (400 MHz, CD_3OD, 25 °C) δ = 7.40 (d, *J* = 8.0 Hz, 4H), 7.18 (d, *J* = 8.1, 4H), 6.96 – 6.89 (m, 8H), 6.86 – 6.79 (m, 8H), 6.72 (s, 4H), 3.48 (d, *J* = 13.0 Hz, 4H), 3.39 – 3.26 (m, 8H), 3.10 – 2.98 (m, 12H), 2.84 (dd, *J* = 14.3, 7.7 Hz, 4H), 1.02 (s, 18H).;^{13}C{^{1}H} NMR (400 MHz, CD_3OD, 25 °C) δ =

176.8, 154.5, 143.0, 138.1, 128.7, 126.6, 125.1, 124.7, 122.5, 119.9, 119.5, 112.4, 111.2, 63.6, 50.3, 39.9, 34.7, 32.1, 29.8; FT-IR (ATR): 3404, 3307, 3057, 2955, 1654, 1524, 1457 cm^{-1}. MS-ESI(+) m/z: 1213.7 ($[M + H]^+$); 1235.9 ($[M + Na]^+$).

Syntheses of the organometallic pseudopeptidic complexes

Synthesis of 1

Ligand **L1** (0.150 g, 0.165 mmol, 1 eq.) was dissolved in 2 mL of MeOH. ZnI_2 (0.105 g, 0.330 mmol, 2 eq.) was dissolved in 0.6 mL of MeOH. The solution of the ligand was added to the ZnI_2 solution, leading to the appearance of abundant white precipitate. The white solid was filtered-off using a syringe filter and the resultant colourless solution was dried under reduced pressure and at 45 ºC to yield pure **1-I** as a white solid (0.175 g, 0.145 mmol, 88% yield). Characterisation: ^{1}H NMR (400 MHz, DMSO-d_6, 25 ºC) δ = 8.58 (s, 4H), 6.86 (s, 4H), 4.71 (d, *J* = 13.1 Hz, 4H), 3.82 (d, *J* = 7.3 Hz, 4H), 3.76 (dd, *J* = 13.5, 3.5 Hz, 4H), 3.25 – 3.18 (m, 8H), 2.94 (d, *J* = 12.4 Hz, 4H), 2.24 – 2.12 (m, 4H), 1.03 (d, *J* = 6.9 Hz, 12H), 0.85 (d, *J* = 6.9 Hz, 12H); ^{13}C{^{1}H} NMR (400 MHz, DMSO-d_6, 25 ºC) δ = 174.7, 160.4, 136.5, 128.4, 120.7, 59.6, 53.2, 41.2, 32.4, 31.5, 19.5, 16.7; FT-IR (ATR): 3456, 3249, 3084, 2959, 1624, 1546, 1480 cm^{-1}. HRMS (ESI+) m/z: $[M]^{2+}$ calcd 495.7353, found 495.7359. See ESI for 2D-NMR analyses (Figure S24-S28).

Synthesis of 2

2-I was synthesized following the protocol described for **L1** but using **L2** as ligand (white solid, 0.422 g, 0.269 mmol, 89% yield). Characterisation: ^{1}H NMR (400 MHz, THF-d_8, 25 ºC) δ = 7.77 (d, *J* = 7.6 Hz, 4H), 7.69 (d, *J* = 7.2 Hz, 8H), 7.24 – 7.14 (m, 12H), 5.95 (s, 4H), 5.71 – 5.57 (m, 4H), 4.60 (d, *J* = 13.5 Hz, 4H), 3.70 – 3.56 (m, 8H), 3.42 – 3.32 (m, 4H), 2.90 (t, *J* = 9.3 Hz, 8H), 2.67 (dd, *J* = 13.5, 3.3 Hz, 4H), 1.09 (s, 18H).;^{13}C{^{1}H} NMR (400 MHz, THF-d_8, 25 ºC) δ = 175.8, 160.9, 138.7, 136.2, 130.3, 128.4, 128.1, 126.3, 121.4, 57.6, 51.8, 41.4, 39.4, 33.1, 31.1; FT-IR (ATR): 3417, 3200, 2949, 1626, 1556, 1480 cm^{-1}. HRMS (ESI+) m/z: $[M]^{2+}$ calcd 591.7353, found 591.7362. See ESI for 2D-NMR analyses (Figures S29-S33).

Synthesis of 3

3-I was synthesized following the protocol described for **L1** but using **L3** as ligand (white solid, 0.134 g, 0.093 mmol, 86% yield). Characterisation: ^{1}H NMR (400 MHz, THF-d_8, 25 ºC) δ = 7.77 (d, *J* = 7.6 Hz, 4H), 7.69 (d, *J* = 7.2 Hz, 8H), 7.24 – 7.14 (m, 12H), 5.95 (s, 4H), 5.71 – 5.57 (m, 4H), 4.60 (d, *J* = 13.5 Hz, 4H), 3.70 – 3.56 (m, 8H), 3.42 – 3.32 (m, 4H), 2.90 (t, *J* = 9.3 Hz, 8H), 2.67 (dd, *J* = 13.5, 3.3 Hz, 4H), 1.09 (s, 18H).;^{13}C{^{1}H} NMR (400 MHz, THF-d_8, 25 ºC) δ = 175.8, 160.9, 138.7, 136.2, 130.3, 128.4, 128.1, 126.3, 121.4, 57.6, 51.8, 41.4, 39.4, 33.1, 31.1; FT-IR (ATR): 3417, 3200, 2949, 1626, 1556, 1480 cm^{-1}. HRMS (ESI+) m/z: $[M]^{2+}$ calcd 591.7353; found 591.7362. See ESI for 2D-NMR analyses (Figures S29-S33).

Synthesis of 4

4-I was synthesized following the protocol described for **1-I** but using **L4** as ligand (white solid, 0.052 g, 0.033 mmol, 82% yield). Characterisation: ^{1}H NMR (400 MHz, THF-d_8, 25 ºC) δ = 9.92 (s, 4H), 8.19 (s, 4H), 7.55 (d, *J* = 2.5 Hz, 4H), 7.38 (d, *J* = 7.9 Hz, 4H), 7.23 (d, *J* = 8.1 Hz, 4H), 6.90 (t, *J* = 7.6 Hz, 4H), 6.73 (t, *J* = 7.5 Hz, 4H), 5.64 (s, 4H), 5.24 (d, *J* = 2.4 Hz, 4H), 4.67 – 4.57 (m, 4H), 3.73 (m, 4H), 3.07 (dd, *J* = 14.1, 4.1 Hz, 4H), 2.90 (dd, *J* = 13.4, 3.4 Hz, 4H), 2.83 (d, *J* = 12.7 Hz, 4H), 0.66 (s, 18H);^{13}C{^{1}H} NMR (400 MHz, THF-d_8, 25 ºC) δ = 176.1, 160.9, 136.7, 128.2, 127.6, 126.9, 121.2, 120.9, 118.6, 118.0, 110.9, 110.2, 56.6, 52.5, 41.3, 32.6, 30.9, 30.1; FT-IR (ATR): 3491, 3428, 3223, 3083, 2959, 1627, 1551, 1478 cm^{-1}. HRMS (ESI+) m/z: $[M]^{2+}$ calcd 669.7571; found 669.7568. See ESI for 2D-NMR analyses (Figures S34-S37).

SUPPLEMENTAL INFORMATION

Document S1. Figures S1–S39, and Tables S1-S6, cartesian coordinates and energies.

ACKNOWLEDGMENTS

This work was supported by the projects UJI-B2019-40 and UJI-B2021-31 (Pla de Promoció de la Investigació de la Universitat Jaume I), AICO/2021/139 (Consellería de Innovació, Universitat, i Ciencia), and PDI2021-124695OB-C22 (FEDER/Ministerio de Ciencia e Innovación–Agencia Estatal de Investigación). Technical support from the SCIC of the UJI is gratefully acknowledged.

AUTHOR CONTRIBUTIONS

Conceptualization: F.E., S.V.L., and E.G.-V.; resources: R.P., B.A., S.V.L., and E.G.-V.; investigation: F.E.; DFT calculations: F.E.; crystal structure refinement: M. B.; writing—

original draft: F.E.; writing—review and editing: F.E., S.V.L. and E.G.-V.; revision of the manuscript: F.E., R.P., M.B., B.A., S.V.L., and E.G.-V.; funding acquisition: B.A., S.V.L., and E.G.-V.; supervision: E.G.-V.

DECLARATION OF INTERESTS

The authors declare no competing interests.

REFERENCES*

1. de Kleijne, K., Hanssen, S. V., van Dinteren, L., Huijbregts, M. A. J., van Zelm, R., and de Coninck, H. (2022). Limits to Paris compatibility of CO_2 capture and utilization. One Earth *5*, 168-185. 10.1016/j.oneear.2022.01.006.
2. Peplow, M. (2022). The race to upcycle CO_2 into fuels, concrete and more. Nature *603*, 780-783. 10.1038/d41586-022-00807-y.
3. Mikkelsen, M., Jorgensen, M., and Krebs, F. C. (2010). The teraton challenge. A review of fixation and transformation of carbon dioxide. Energy Environ. Sci. *3*, 43-81. 10.1039/B912904A.
4. Shi, J., Jiang, Y., Jiang, Z., Wang, X., Wang, X., Zhang, S., Han, P., and Yang, C. (2015). Enzymatic conversion of carbon dioxide. Chem. Soc. Rev. *44*, 5981-6000. 10.1039/C5CS00182J.
5. Long, N.V.D., Lee, J., Koo, K.-K., Luis, P., and Lee, M. (2017). Recent Progress and Novel Applications in Enzymatic Conversion of Carbon Dioxide. Energies *10*, 473. 10.3390/en10040473.
6. Sahoo, P.C., Kumar, M., Puri, S.K., and Ramakuma, S.S.V. (2018). Enzyme inspired complexes for industrial CO2 capture: Opportunities and challenges. J. CO2 Util. *24*, 419-429. 10.1016/j.jcou.2018.02.003.
7. Artz, J., Müller, T. E., Thenert, K., Kleinekorte, J., Meys, R., Sternberg, A., Bardow, A., and Leitner, W. (2018). Sustainable Conversion of Carbon Dioxide: An Integrated Review of Catalysis and Life Cycle Assessment. Chem. Rev. *118*, 434-504. 10.1021/acs.chemrev.7b00435.
8. Moller, F., Piontek, S., Miller, R.G., and Apfel, U.P. (2018). From Enzymes to Functional Materials—Towards Activation of Small Molecules. Chem. Eur. J. *24*, 1471-1493. 10.1002/chem.201703451.
9. Gamba, I. (2018). Biomimetic Approach to CO_2 Reduction. Bioinorganic Chem. Appli. *2018*, 1. 10.1155/2018/2379141.
10. Guo, L., Lamb, K. J., and North, M. (2021). Recent developments in organocatalysed transformations of epoxides and carbon dioxide into cyclic carbonates. Green Chem. *23*, 77-118. doi.org/10.1039/D0GC03465G.
11. North, M., and Pasquale, R. (2009). Mechanism of Cyclic Carbonate Synthesis from Epoxides and CO_2. Angew. Chem. Int. Ed. *48*, 2946-2948. 10.1002/anie.200805451.
12. Pescarmona, P. P. (2021). Cyclic carbonates synthesised from CO2: Applications, challenges and recent research trends. Curr. Opin. Green Sustain. *29*, 100457. 10.1016/j.cogsc.2021.100457.
13. Aomchad, V., Cristòfol, A., Monica, F.D., Limburg, B., D'Elia, V., and Kleij, A. W. (2021). Recent progress in the catalytic transformation of carbon dioxide into biosourced organic carbonates. Green Chem. *23*, 1077-1113. 10.1039/D0GC03824E
14. Whiteoak, C. J., Kielland, N., Laserna, V., Escudero-Adán, E. C., Martin, E., and Kleij, A. W. (2013). A Powerful Aluminum Catalyst for the Synthesis of Highly Functional Organic Carbonates. J. Am. Chem. Soc. *135*, 1228-1231.
15. Mirabaud, A., Mulatier, J.-C., Martinez, A., Dutasta, J. P., and Dufaud, V. (2015). Investigating Host–Guest Complexes in the Catalytic Synthesis of Cyclic Carbonates from Styrene Oxide and CO_2. ACS Catal. *5*, 6748-6752. 10.1021/acscatal.5b01545.
16. Martínez-Rodríguez, L., Garmilla, J. O., and Kleij, A. W. (2016). Cavitand-Based Polyphenols as Highly Reactive Organocatalysts for the Coupling of Carbon Dioxide and Oxiranes. ChemSusChem *9*, 749-755. 10.1002/cssc.201501463.
17. Esteve, F., Altava, B., Burguete, M. I., Bolte, M., García-Verdugo, E., and Luís, S. V. (2020). Pseudopeptidic macrocycles as cooperative minimalistic synzyme systems for the remarkable activation and conversion of CO_2 in the presence of the chloride anion. Green Chem. *22*, 4697-4705. 10.1039/D0GC01449D.
18. Mirabaud, A., Martinez, A., Bayard, F., Dutasta, J.-P., and Dufaud, V. (2018). A new heterogeneous host-guest catalytic system as an eco-friendly approach for the synthesis of cyclic carbonates from CO_2 and epoxides. New J. Chem. *42*, 16863-16874. 10.1039/C8NJ03065K.
19. Ren, W.-M., Wu, G.-P., Lin, F., Jiang, J.-Y., Liu, C., Luo, Y., and Lu, X.-B. (2012). Role of the co-catalyst in the asymmetric coupling of racemic epoxides with CO_2 using multichiral Co(iii) complexes: product selectivity and enantioselectivity. Chem. Sci. *3*, 2094–2102. 10.1039/c2sc20068f.
20. Takaishi, K., Nath, B. D., Yamada, Y., Kosugi H., and Ema, T. (2019). Unexpected Macrocyclic Multinuclear Zinc and Nickel Complexes that Function as Multitasking Catalysts for CO_2 Fixations. Angew. Chem. Int. Ed. *58*, 9984-9988. 10.1002/anie.201904224.
21. Wu, X., Chen, C., Guo, Z., North, M., and Whitwood, A. C. (2019). Metal- and Halide-Free Catalyst for the Synthesis of Cyclic Carbonates from Epoxides and Carbon Dioxide. ACS Catal. *9*, 1895-1906. 10.1021/acscatal.8b04387.
22. Ema, T., Miyazaki, Y., Shimonishi, J., Maeda, C., and Hasegawa, J.-Y. (2014). Bifunctional Porphyrin Catalysts for the Synthesis of Cyclic Carbonates from Epoxides and

CO_2: Structural Optimization and Mechanistic Study. J. Am. Chem. Soc. *136*, 15270–15279. 10.1021/ja507665a.

23. Li, P., and Cao, Z. (2019). Catalytic coupling of CO_2 with epoxide by metal macrocycles functionalized with imidazolium bromide: insights into the mechanism and activity regulation from density functional calculations. Dalton Trans. *48*, 1344-1350. 10.1039/c8dt04684k.
24. Esteve, F., Escrig, A., Porcar, R., Luis, S. V., Altava, B., and García-Verdugo, E. (2022). Immobilized Supramolecular Systems as Efficient Synzymes for CO_2 Activation and Conversion. Adv. Sustainable Syst. *6*, 2100408. 10.1002/adsu.202100408.
25. Desens, W., Kohrt, C., Frank, M., and Werner, T. (2015). Highly Efficient Polymer-Supported Catalytic System for the Valorization of Carbon Dioxide. ChemSusChem *8*, 3815-3822. 10.1002/cssc.201501119.
26. Hao, Y., Yan, X., Chang, T., Liu, X., Kang, L., Zhu, Z., Panchal, B., and Qin, S. (2022). Hydroxyl-anchored covalent organic crown-based polymers for CO_2 fixation into cyclic carbonates under mild conditions. Sustain. Energy Fuels *6*, 121-127. 10.1039/d1se01120k.
27. Longwitz, L., Steinbauer, J., Spannenberg, A., and Werner, T. (2017). Calcium-Based Catalytic System for the Synthesis of Bio-Derived Cyclic Carbonates under Mild Conditions. ACS Catal. *8*, 665-672. 10.1021/acscatal.7b03367.
28. Maeda, C., Mitsuzane, M., and Ema, T. (2019). Chiral Bifunctional Metalloporphyrin Catalysts for Kinetic Resolution of Epoxides with Carbon Dioxide. Org. Lett. *21*, 1853–1856. 10.1021/acs.orglett.9b00447.
29. Cavalleri, M., Panza, N., di Biase, A., Tseberlidis, G., Rizzato, S., Abbiati, G., and Caselli, A. (2021). [Zinc(II)(Pyridine-Containing Ligand)] Complexes as Single-Component Efficient Catalyst for Chemical Fixation of CO_2 with Epoxides. Eur. J. Org. Chem. *19*, 2764-2771. 10.1002/ejoc.202100409.
30. Olivo, G., Capocasa, G., Del Giudice, D., Lanzalunga, O. Di Stefano, S. (2021), New horizons for catalysis disclosed by supramolecular chemistry, *Chem. Soc. Rev*. 50, 7681-7724. 10.1039/D1CS00175B.
31. Esteve, F., Altava, B., García-Verdugo, E., Luis, S.V., and Lehn, J.-M. (2022). Doubly chiral pseudopeptidic macrobicyclic molecular cages: Water-assisted dynamic covalent self-assembly and chiral self-sorting. Chem *8*, 2023-2042. 10.1016/j.chempr.2022.04.007.
32. Becerril, J., Bolte, M., Burguete, M. I., Galindo, F., Garcia-España, E., Luis, S. V., and Miravet, J. F. (2003). Efficient Macrocyclization of U-Turn Preorganized Peptidomimetics: The Role of Intramolecular H-Bond and Solvophobic Effects. J. Am. Chem. Soc. *125*, 6677-6686. 10.1021/ja0284759.
33. Esteve, F., Altava, B., Bolte, M., Burguete, M. I., García-Verdugo E., and Luis, S. V. (2020). Highly Selective Anion Template Effect in the Synthesis of Constrained Pseudopeptidic Macrocyclic Cyclophanes. J. Org. Chem. *85*, 1138-1145. 10.1021/acs.joc.9b03048.
34. Martí-Centelles, V., Pandey, M. D., Burguete, M. I., and Luis, S. V. (2015). Macrocyclization Reactions: The Importance of Conformational, Configurational, and Template-Induced Preorganization. Chem. Rev. *115*, 8736-8834. 10.1021/acs.chemrev.5b00056.
35. Alvarez, S. (2013). A cartography of the van der Waals territories. Dalton Trans. *42*, 8617-8636. 10.1039/c3dt50599e.
36. Kember, M. R., White, J. P., and Williams, C. K. (2009). Di- and Tri-Zinc Catalysts for the Low-Pressure Copolymerization of CO_2 and Cyclohexene Oxide. Inorg. Chem. *48*, 9535–9542. 10.1021/ic901109e.
37. Deacy, A. C., Durr, C. B., and Williams, C. K. (2020). Heterodinuclear complexes featuring Zn(ii) and M = Al(iii), Ga(iii) or In(iii) for cyclohexene oxide and CO_2 copolymerisation. Dalton Trans. *49*, 223-231. 10.1039/c9dt02918d.
38. Nicolaou, K. C., Couladouros, E. A., Nantermet, P. G., Renaud, J., Guy, R. K., and Wrasidlo, W. (1994). Synthesis of C-2 Taxol Analogues. Angew. Chem. Int. Ed. Engl. *33*, 1581-1583. 10.1002/anie.199415811.
39. Song, C. E., and Lee, S.-G. (2002). Supported Chiral Catalysts on Inorganic Materials. Chem. Rev. *102*, 3495–3524. 10.1021/cr0103625.
40. Kang, S. K., Jeon, J. H., Nam, K. S., Park, C. H., and Lee, H. W. (1994). Regioselective Protection of Triols to Cyclic Carbonates. Synth. Commun. *24*, 305-312. 10.1080/00397919408011189.
41. Matsumoto, K., Fuwa, S., and Kitajima, H. (1995). Enzyme-mediated enantioselective hydrolysis of cyclic carbonates. Tetrahedron Lett. *36*, 6499-6502. 10.1016/S0040-4039(02)01628-3.
42. Zhou, H., Zhang, H., Mu, S., Zhang, W.-Z., Ren, W.-M., and Lu, X.-B. (2019). Highly regio- and stereoselective synthesis of cyclic carbonates from biomass-derived polyols via organocatalytic cascade reaction. Green Chem. *21*, 6335–6341. 10.1039/c9gc03013a.
43. North, M., Quek, S. C. Z., Pridmore, N. E., Whitwood, A. C., and Wu, X. (2015). Aluminum(salen) Complexes as Catalysts for the Kinetic Resolution of Terminal Epoxides via CO_2 Coupling. ACS Catal. *5*, 3398–3402. 10.1021/acscatal.5b00235.
44. Maeda, C., Ogawa, K., Sadanaga, K., Takaishi, K., and Ema, T. (2019). Chiroptical and catalytic properties of doubly binaphthyl-strapped chiral porphyrins. Chem. Commun. *55*, 1064-1067. 10.1039/c8cc09114e.
45. Fu, X., Jing, X., Jin, L., Zhang, L., Zhang, X., Hu, B., and Jing, H. (2018). Chiral basket-handle porphyrin-Co complexes for the catalyzed asymmetric cycloaddition of CO_2 to epoxides.

Chin. J. Catal. *39*, 997-1003. 10.1016/S1872-2067(18)63023-2.

46. Liu, S., Suematsu, N., Maruoka, K., and Shirakawa, S. (2016). Design of bifunctional quaternary phosphonium salt catalysts for CO_2 fixation reaction with epoxides under mild conditions. Green Chem. *18*, 4611-4615. 10.1039/c6gc01630h.
47. Ema, T., Yokoyama, M., Watanabe, S., Sasaki, S., Ota, H., and Takaishi, K. (2017). Chiral Macrocyclic Organocatalysts for Kinetic Resolution of Disubstituted Epoxides with Carbon Dioxide. Org. Lett. *19*, 4070-4073. 10.1021/acs.orglett.7b01838.
48. Roy, T., Kureshy, R. I., Khan, N. H., Abdi, S. H. R., and Bajaj, H. C. (2013). Asymmetric cycloaddition of CO_2 and an epoxide using recyclable bifunctional polymeric Co(iii) salen complexes under mild conditions. Catal. Sci. Technol. *3*, 2661-2667. 10.1039/c3cy00325f.
49. Ren, W.-M., Liu, Y., and Lu, X.-B. (2014). Bifunctional Aluminum Catalyst for CO2 Fixation: Regioselective Ring Opening of Three-Membered Heterocyclic Compounds. J. Org. Chem. *79*, 9771-9777. 10.1021/jo501926p.
50. Al-Qaisi, F. M., Nieger, M., Kemell, M. L., and Repo, T. J. (2016). Catalysis of Cycloaddition of Carbon Dioxide and Epoxides Using a Bifunctional Schiff Base Iron(III) Catalyst. ChemistrySelect *3*, 545-548. 10.1002/slct.201600162.
51. Clegg, W., Harrington, R. W., and North, M. (2010). Cyclic Carbonate Synthesis Catalysed by Bimetallic Aluminium–Salen Complexes. Chem. Eur. J. 16, 6828-6843. 10.1002/chem.201000030.
52. Gorla, L., Martí-Centelles, V., Altava, B., Burguete, M. I., Luis, S. V. (2019). The role of the side chain in the conformational and self-assembly patterns of C_2-symmetric Val and Phe pseudopeptidic derivatives. CrystEngComm *21*, 2398-2408. 10.1039/c8ce02088d.
53. Reichardt, C. (2003). Solvents and Solvent Effects in Organic Chemistry (Wiley-VCH Publishers).
54. Kelly, S. M., Jess, T. J., and Price, N. C. (2005). How to study proteins by circular dichroism. Biochim. Biophys. Acta *1751*, 119-139. 10.1016/j.bbapap.2005.06.005.
55. Wang, L., Zhang, G., Kodama, K., and Hirose, T. (2016). An efficient metal- and solvent-free organocatalytic system for chemical fixation of CO_2 into cyclic carbonates under mild conditions. Green Chem. *18*, 1229-1233. 10.1039/c5gc02697k.
56. Notni, J., Schenk, S., Görls, H., Breitzke, H., and Anders, E. (2008). Formation of a Unique Zinc Carbamate by CO_2 Fixation: Implications for the Reactivity of Tetra-Azamacrocycle Ligated Zn(II) Complexes. Inorg. Chem. *47*, 1382-1390. 10.1021/ic701899u.
57. Siegelman, R. L., McDonald, T. M., Gonzalez, M. I., Martell, J. D., Milner, P. J., Mason, J. A., Berger, A. H., Bhown, A. S., and Long, J. R. (2017). Controlling Cooperative CO_2 Adsorption in Diamine-Appended Mg2(dobpdc) Metal–Organic Frameworks. J. Am. Chem. Soc. *139*, 10526-10538. 10.1021/jacs.7b05858.
58. Castro-Gómez, F., Salassa, G., Kleij, A. W., and Bo, C. (2013). A DFT Study on the Mechanism of the Cycloaddition Reaction of CO_2 to Epoxides Catalyzed by Zn(Salphen) Complexes. Chem. Eur. J. *19*, 6289–6298. 10.1002/chem.201203985.
59. Esteve, F., Altava, B., Luis, S. V., and García-Verdugo, E. (2022). Basically, nucleophilicity matters little: towards unravelling the supramolecular driving forces in enzyme-like CO2 conversion. Org. Biomol. Chem. *20*, 6637-6645. 10.1039/d2ob00948j.
60. Jennings, W. B., Farrell, B. M., and Malone, J. F. (2001). Attractive Intramolecular Edge-to-Face Aromatic Interactions in Flexible Organic Molecules. Acc. Chem. Res. *34*, 885–894. 10.1021/ar0100475.
61. Frassineti, C., Ghelli, S., Gans, P., Sabatini, A., Moruzzi, M.S., and Vacca, A. (1995). Nuclear Magnetic Resonance as a Tool for Determining Protonation Constants of Natural Polyprotic Bases in Solution. Analytical Biochemistry *231*, 374-382. 10.1006/abio.1995.9984.
62. Sheldrick, G. M. (2008). A short history of SHELX. Acta Crystallogr., Sect. A: Found. Crystallogr. *64*, 112-122. 10.1107/S0108767307043930.
63. Sheldrick, G. M. (2015). Crystal structure refinement with SHELXL. Acta Crystallogr., Sect. C: Struct. Chem. *71*,3-8. 10.1107/S2053229614024218.
64. Macrae, C. F., Bruno, I. J., Chisholm, J. A., Edgington, P. R., McCabe, P., Pidcock, E., Rodriguez-Monge, L., Taylor, R., van de Streek, J., and Wood, P. A. (2008). Mercury CSD 2.0 – new features for the visualization and investigation of crystal structures. J. Appl. Crystallogr. *41*, 466-470. 10.1107/S0021889807067908.
65. A Frisch, M. J., Trucks, G. W., Schlegel, H. B., Scuseria, G. E., Robb, M. A., Cheeseman, J. R., Scalmani, G., Barone, V., Mennucci, B., Petersson, G. A., et al. (2010). Gaussian 09, Revision B.01 (Gaussian, Inc).
66. Becke, A. D. (1993). Density - functional thermochemistry. III. The role of exact exchange. J. Chem. Phys. *98*, 5648-5652. 10.1063/1.464913.
67. Chiodo, S., and Sicilia, E. (2006). LANL2DZ basis sets recontracted in the framework of density functional theory. J. Chem. Phys. *125*, 104107. 10.1063/1.2345197.